Effect of composition on damage accumulation in ternary ZnO-based oxides implanted with heavy ions

A. Yu. Azarov, , B. G. Svensson, , A. Hallén, , X. L. Du, and , and A. Yu. Kuznetsov

Citation: Journal of Applied Physics **108**, 033509 (2010); doi: 10.1063/1.3467532
View online: http://dx.doi.org/10.1063/1.3467532
View Table of Contents: http://aip.scitation.org/toc/jap/108/3
Published by the American Institute of Physics

AIP | Journal of Applied Physics
Save your money for your research.
It's now FREE to publish with us -
no page, color or publication charges apply.
Publish your research in the
Journal of Applied Physics
to claim your place in applied
physics history.

Effect of composition on damage accumulation in ternary ZnO-based oxides implanted with heavy ions

A. Yu. Azarov,[1,a)] B. G. Svensson,[1] A. Hallén,[2] X. L. Du,[3] and A. Yu. Kuznetsov[1]
[1]*Department of Physics, University of Oslo, P.O. Box 1048 Blindern, NO-0316 Oslo, Norway*
[2]*KTH-ICT, Royal Institute of Technology, Electrum 229, SE-164 40 Kista-Stockholm, Sweden*
[3]*Institute of Physics, The Chinese Academy of Sciences, Beijing 100190, China*

(Received 25 March 2010; accepted 28 June 2010; published online 4 August 2010)

Thin films of wurtzite $Mg_xZn_{1-x}O$ ($x \leq 0.3$) grown by molecular beam epitaxy and wurtzite $Cd_xZn_{1-x}O$ ($x \leq 0.05$) grown by metal organic chemical vapor deposition were implanted at room temperature with 150 keV Er^+ ions and 200 keV Au^+ ions in a wide dose range. Damage accumulation was studied by Rutherford backscattering/channeling spectrometry. Results show that the film composition affects the damage accumulation behavior in both MgZnO and CdZnO dramatically. In particular, increasing the Mg content in MgZnO results in enhanced damage accumulation in the region between the bulk and surface damage peaks characteristically distinguished in the pure ZnO. However, the overall damage accumulation in MgZnO layers, as well as in pure ZnO, exhibits saturation with increasing ion dose and MgZnO cannot be amorphized even at the highest ion dose used (3×10^{16} Er/cm^2). Increasing the Cd content in CdZnO affects the saturation stage of the damage accumulation and leads to an enhancement of damage production in both Cd and Zn sublattices. © *2010 American Institute of Physics*. [doi:10.1063/1.3467532]

I. INTRODUCTION

Zink oxide (ZnO) is a direct band-gap semiconductor with numerous promising applications in the field of short wavelength optoelectronics[1,2] on behalf of its wide band gap ($E_g \sim 3.4$ eV) and large exciton binding energy (~ 60 meV) at room temperature. Band-gap engineering is one of the key issues for the formation of heterostructures and quantum wells, which are needed for fabrication of modern devices. It is established that the band gap of ZnO can be tuned up/down by alloying with other group-II oxides, such as MgO ($E_g \sim 7.8$ eV) and CdO ($E_g \sim 2.3$ eV or smaller for indirect transitions). For example, in Refs. 3 and 4 it was reported that band-gap energy of wurtzite ternary ZnO-based compounds can be tuned from ~ 1.85 to ~ 3.9 eV by appropriate Cd or Mg incorporation. However, the crystalline quality of the MgZnO and CdZnO films and, hence, the utilization of this material for optical applications, is challenged by a phase separation at high Mg and Cd concentrations.[5–7] The phase separation is possible due to the fact that the binary components have different crystal structures (ZnO has a hexagonal wurtzite (W) structure, while MgO and CdO exhibit a rock-salt (RS) cubic structure in equilibrium) demonstrating low the thermodynamic solubility of RS-MgO and RS-CdO in W-ZnO.[3] This also implies that the fabrication of single-phase W-MgZnO and W-CdZnO films with high concentrations of Mg and Cd is possible by employing metastable synthesis conditions only.

Ion implantation is a very attractive technological tool for semiconductor device processing and it can be used to introduce controllable impurity concentrations at a precise depth below the surface. However, the bombardment with energetic ions inevitably produces defects which often undesirably affect the device performance. Concurrently, it has been shown that ZnO exhibits an extremely strong degree of dynamic annealing (i.e., defect migration and recombination processes occurring during the ion implantation) even at low irradiation temperatures and this material is more radiation resistant than its major rival GaN.[2,8] For example, previous studies have shown that ZnO cannot be amorphized with heavy ions, such as Au (Ref. 8) and Bi (Ref. 9), even at very high ion doses where each lattice atom is displaced up to hundred times. Also for implantation at liquid nitrogen temperature, where the self annealing during implantation is supposed to be very low due to the slower diffusion of lattice defects, it is difficult to make the ZnO crystals amorphous.[8] Moreover, the damage accumulation in ZnO, as well as the removal of radiation defects during postimplantation annealing, can be strongly affected by the chemical nature of the implanted species.[8,10]

However, despite intensive studies of ion-beam related phenomena in ZnO during the last decade,[2,8–11] our knowledge about mechanisms of radiation damage formation in this material is still far from being mature. Furthermore, there is very little known about radiation damage formation in ZnO-based ternary oxides, e.g., MgZnO and CdZnO. In fact the incorporation of third element in a binary compound can dramatically affect both the level of implantation disorder and the main features of damage accumulation behavior. For example, comparing to ternary GaN-based nitrides, an increase in Al concentration strongly enhances dynamic annealing processes in AlGaN (Ref. 12). In contrast, an increase in In content suppresses dynamic annealing processes and leads to the enhancement of damage production in InGaN films.[12,13] Moreover, both AlGaN and InGaN exhibit no characteristic surface amorphization under ion bombardment in a contrast to pure GaN (Ref. 12). An understanding of

[a)]Electronic mail: a.y.azarow@smn.uio.no.

 © 2010 American Institute of Physics

radiation effects in MgZnO and CdZnO films is important for a successful ion-beam processing of ZnO-based devices.

In this report, we present pioneering results indicating that the Mg and Cd composition strongly affect the damage accumulation behavior in MgZnO and CdZnO films implanted with heavy ions.

II. EXPERIMENTAL

About 1 μm thick single-phase $Mg_xZn_{1-x}O$ (x=0, 0.1, and 0.3) layers were grown by molecular beam epitaxy on α-Al_2O_3 substrates. Similarly ~1 μm thick $Cd_xZn_{1-x}O$ (x=0.012 and 0.05) layers were synthesized by metal organic chemical vapor deposition. According to x-ray diffraction measurements, all as-grown MgZnO and CdZnO samples exhibit single-phase wurtzite structure without any indication of phase separation. The MgZnO samples were implanted with 150 keV $^{166}Er^+$ ions using an ion flux of 2.5×10^{12} cm^{-2} s^{-1} in a dose range of 1×10^{14}–3×10^{16} cm^{-2}. The CdZnO samples were implanted with 200 keV Au^+ ions using an ion flux of 1×10^{12} cm^{-2} s^{-1} to ion doses of 5×10^{14} and 5×10^{15} cm^{-2}. In order to distinguish how the Cd content affects the damage buildup in CdZnO layers, a set of control hydrothermally grown ZnO single crystal samples were subjected to similar implants. All implantations were carried out at room temperature at 7° off the [0001] direction in order to reduce channeling.

Implantation-induced disorder was measured by Rutherford backscattering/channeling spectrometry (RBS/C) with 2 MeV $^4He^+$ ions incident along the [0001] direction and backscattered into detectors at 170° and 100° relative to the incident beam direction. The 100°, so-called glancing-angle detector, geometry was used to provide enhanced depth resolution for examining near-surface damage accumulation. The 170° geometry was used to provide enhanced mass resolution to separate signals from Cd and Zn atoms, which is needed to accurately examine the damage-depth profiles in both the Cd and Zn sublattice[14] of CdZnO layers. Although the RBS/C technique reveals primarily interstitial (displaced) atoms it is very difficult to draw any conclusion about the type of defects presented in the sample based on RBS results alone. Even open volume defects like vacancies and vacancy clusters induce local stress and contribute to the backscattering yield during RBS/C analysis. Therefore, all RBS/C spectra were analyzed with one of the conventional algorithms[15] for extracting the effective number of so-called scattering centers, conventionally referred below as "relative disorder."

III. RESULTS AND DISCUSSION

A. ZnO

Figure 1 shows RBS/C spectra (a) and disorder-depth profiles (b) of ZnO implanted at room temperature with $^{166}Er^+$ ions using different doses. The peak in the RBS/C spectra for channel numbers more then 320 is related to a signal from implanted Er atoms. It is seen from this figure that in pure ZnO, the damage accumulates both at the surface and deeper in the bulk of the film (most pronounced for 2×10^{15} and 5×10^{15} cm^{-2} ion doses). The depth where the nuclear energy loss is maximum (R_{pd}) and the mean projected range (R_p) of 150 keV Er ions in ZnO were found at 21 nm and 33 nm, respectively [see Fig. 1(c)] in accordance with TRIM code[16] simulations. It is seen that the actual position of the bulk damage peak is considerably deeper than R_{pd} and close to R_p for the low ion doses. Furthermore, the damage in the film expands to larger depths and exhibits a saturation trend with increasing ion dose. Interestingly, there is a "valley" in the damage profile at R_{pd}, i.e., the region where primary defects are generated, as clearly seen for intermediate doses in Fig. 1(b). Such complexity in the damage accumulation is typical for crystals with a large degree of ionicity of the chemical bonds.[17]

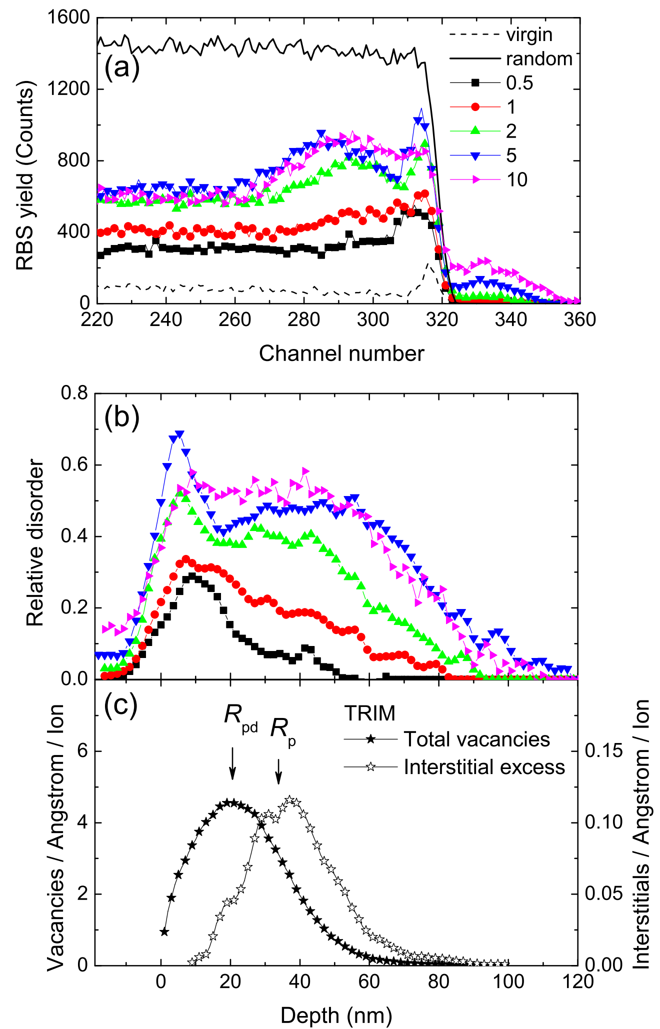

FIG. 1. (Color online) The RBS/C spectra (a) and depth profiles of relative disorder in Zn sublattice (b) of pure ZnO bombarded at room temperature by 150 keV $^{166}Er^+$ ions with ion flux of 2.5×10^{12} cm^{-2} s^{-1}. Implantation doses (in 10^{15} ions $\times$ cm^{-2}) are indicated. A virgin spectrum is shown in (a) for comparison. Profiles of Er-ion-generated lattice vacancies and interstitial excesses (incident Er ions are also included) predicted by TRIM simulations are shown in (c).

The observed damage accumulation behavior in ZnO may be attributed to the dynamic annealing processes in ZnO during ion bombardment as well as a large role of both the implanted species and the surface, which is considered to be a strong unsaturated sink for the generated mobile point defects. Indeed, an extremely pronounced radiation hardness of ZnO even at low temperatures suggests that the major part of

the ion-beam-generated defects effectively annihilate during the irradiation. The minor effect of implantation temperature on defect formation in ZnO (Ref. 8) indicates extremely low activation of these processes. It is also well known that vacancies and interstitials are spatially separated in a collision cascade,[18] with an excess of interstitial close to the ion projected range and a vacancy excess closer to the surface. Evidently, dynamic annealing processes should be more efficient in the region where the spatial overlap of vacancy and interstitial distributions is larger. The effect of spatial separation of vacancies and interstitials during ion bombardment is illustrated by Fig. 1(c), which shows the depth profiles of excess interstitials (incident Er ions are also included) and ion-generated vacancies calculated with the TRIM code[16] with effective threshold energies for atomic displacements of 34 eV and 44 eV for Zn and O sublattices, respectively.[19] Comparing Figs. 1(b) and 1(c) it is seen that a significant part of integral disorder in Fig. 1(b) is located deeper in the film (at least for the higher dose implants) correlating with the excess interstitial profile.

In its turn, the residual damage observed either at the surface or deep into the film should be formed by defects that survived the initial stages of dynamic annealing and diffused from the region where they were generated. Note that, although the long-range diffusion of generated defects should be suppressed in the damaged crystal, the bulk damage increases likely due to defects which are generated in the deep tail of their depth distribution, where dynamic annealing processes are not efficient.

Another feature seen from Fig. 1 is that the surface damage peak for the lowest ion dose is broader than that for higher doses. This interesting behavior of the surface damage peak for pure ZnO may be attributed to the formation of a new damage peak between the surface and "bulk" damage peak. The appearance of this intermediate damage peak, has been observed in ZnO for heavy[8] and cluster ion[20] irradiation and has been attributed to effects of high densities of collision cascades.

Thus, the damage buildup and its evolution in pure ZnO exhibit a complex behavior as a function of ion dose. More work and additional analysis techniques are needed to better understand the exact role of end-of-range defects, chemical effects of the implanted impurities, defect diffusion, and material decomposition in the evolution of the bulk damage peak in ZnO. In spite the complexity may increase in ternary ZnO-based alloys we are below presenting the results of our pioneering measurements in order to introduce the topic and initiate the discussion.

B. MgZnO

Figure 2 shows RBS/C spectra of $Mg_{0.3}Zn_{0.7}O$ films implanted under the same irradiation conditions as the pure ZnO samples in Sec. III A. Magnesium at the surface can be seen as a small step in the random spectrum at channel 243, in good agreement with simulations. It is clearly seen from this figure that by increasing the Mg content in $Mg_xZn_{1-x}O$ film the damage buildup behavior is dramatically affected. As illustrated in Fig. 2 for x=0.3, the damage buildup appears unimodal, i.e., no clear separation between the bulk peak and the surface damage peaks is observed in contrast to that in Fig. 1(a). The effect of Mg content on the damage buildup is further illustrated by Fig. 3, which compares the depth profiles of relative disorder in the Zn sublattice for samples with different Mg content that are implanted to the same ion dose of 5×10^{15} cm^{-2} (Ref. 21). It is clearly seen that an increase in the Mg content strongly enhances the damage accumulation in the region between the bulk and surface damage peaks, labeled with arrows in Fig. 3. However, despite of the remarkable increase in the damage production in $Mg_xZn_{1-x}O$ films with increasing Mg content, the overall damage level in $Mg_xZn_{1-x}O$, as well as in ZnO, exhibits a saturation at high ion doses and does not reach the random level even for the highest ion dose used (3×10^{16} cm^{-2}).

Figure 4 shows the maximum relative disorder in the bulk damage peak as a function of ion dose for all MgZnO samples studied[22] demonstrating a clear saturation trend. Note, increasing the Mg content does not change the general trend of the damage accumulation in the bulk, but leads to an enhancement either in the damage production efficiency, or

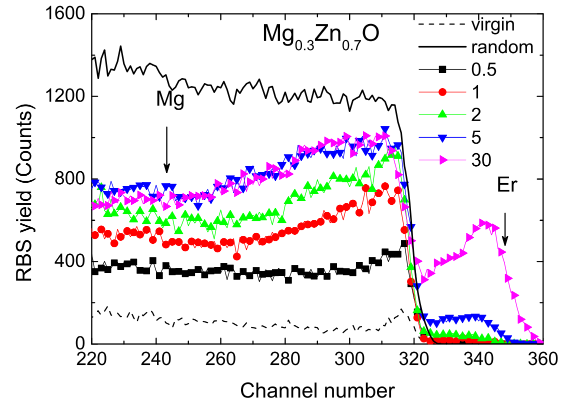

FIG. 2. (Color online) The RBS/C spectra of $Mg_{0.3}Zn_{0.7}O$ bombarded at room temperature by 150 keV $^{166}Er^+$ ions with ion flux of 2.5×10^{12} cm^{-2} s^{-1}. Implantation doses (in 10^{15} ions$\times$cm^{-2}) are indicated. The positions of Mg and Er at the film surface are indicated by the arrows. A virgin spectrum is shown for comparison.

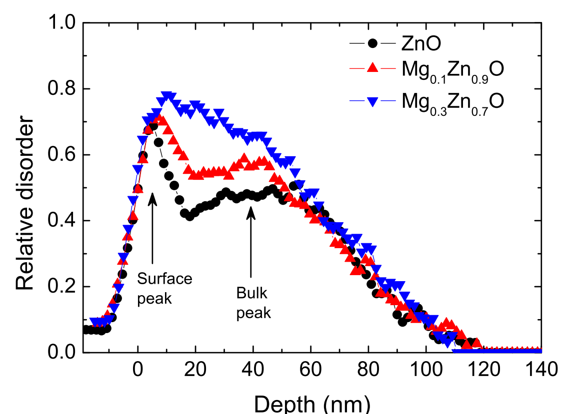

FIG. 3. (Color online) Comparison of depth profiles of relative disorder in Zn sublattice (extracted from RBS/C spectra) in $Mg_xZn_{1-x}O$ (x=0, 0.1, and 0.3) bombarded at room temperature with 150 keV $^{166}Er^+$ ions to an ion dose of 5×10^{15} cm^{-2}.

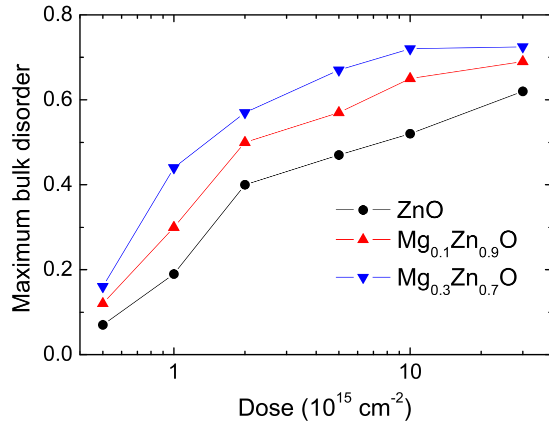

FIG. 4. (Color online) The ion dose dependence of the maximum relative disorder in the bulk defect peak in $Mg_xZn_{1-x}O$ (x=0, 0.1, and 0.3) bombarded at room temperature by 150 keV $^{166}Er^+$ ions.

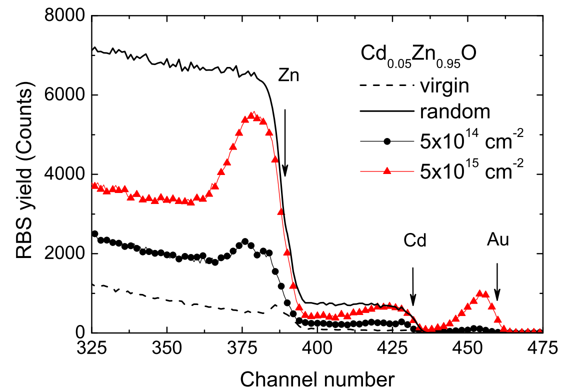

FIG. 5. (Color online) The RBS/C spectra of $Cd_{0.05}Zn_{0.95}O$ bombarded at room temperature with 200 keV Au^+ ions to two different ion doses as indicated in the legend. The positions of Cd, Zn, and Au at the film surface are indicated by the arrows. The virgin spectrum is also shown for comparison.

the damage saturation level from 0.45 to 0.7 for ZnO and $Mg_{0.3}Zn_{0.7}O$, respectively. Importantly, in spite of increasing disorder no amorphization is detected in heavy ion implanted $Mg_xZn_{1-x}O$ ($x \leq 0.3$), which indicates that a strong dynamic annealing process takes place.

Previous studies of defect microstructure in ion-implanted ZnO revealed that the bulk damage peak may be attributed to a high density of stable planar defects in addition to defect clusters. These planar defects (stacking faults) are parallel to the basal plane of the ZnO wurtzite structure.[8,23] The similarity of damage accumulation behavior in ZnO and MgZnO may indicate the same nature of the disorder appearing in the bulk of the films. However, the disorder enhancement in the region between the bulk and surface damage peaks with increasing Mg content may indicate changing surface-defect interaction conditions comparing to that in pure ZnO. It is important to note that the damage level at the surface is almost independent on the Mg content and also exhibits a saturation effect.

Considering the aspects that may influence the results in Fig. 3 we may mention strain and phase stability effects. First, strain-induced effects originating from the lattice mismatch between a sapphire substrate and a film may potentially influence the damage accumulation behavior in MgZnO. However, it has been shown that MgZnO films exhibit relatively small alteration of the lattice parameters with a variation in Mg content used in our experiments.[3] Therefore, strain-induced effects should not affect the damage accumulation in MgZnO in the first place. Second, the enhanced damage production in MgZnO films may be also related to the phase instability of this material during ion bombardment. Indeed, as it has been mentioned in Sec. I, W-MgZnO films are metastable at high Mg content, so that W-ZnO and RS-MgO may potentially segregate during the implantation. It is seen from Figs. 3 and 1(c) that the enhancement of damage production occurs at the depth of R_{pd}, i.e., in the region where nuclear energy loss of impinging atoms is at maximum. Evidently, the phase separation is more likely to occur in the regions where the defect generation rate is maximized and this mechanism may be more pronounced for the bombardment of MgZnO with heavier ions, which produce denser collision cascades.

Further, the damage accumulation in MgZnO layers may be also affected by the initial crystal quality. The minimum channeling yield is 3%, 5%, and 6% for the as-grown ZnO, $Mg_{0.1}Zn_{0.9}O$ and $Mg_{0.3}Zn_{0.7}O$ samples, respectively, which indicates a lowering of the crystal quality of the material with increasing Mg concentration. These initially presented defects may potentially act as additional nucleation sites for the defect growth and/or affect diffusion length of primary defects and, hence, give some contribution to the damage enhancement in material with increasing the Mg content.

It is important to note that the damage accumulation in MgZnO is also different from that occurring in MgO (Refs. 24 and 25). Indeed, although the disorder in MgO exhibits typical feature for the ionic crystals with damage saturation, the ion-beam-produced damage in MgO accumulates preferentially in the bulk. Furthermore, the damage saturation level in MgO is lower than that for ZnO and MgZnO (Ref. 25). Such damage accumulation behavior may be attributed to the lower ionicity of Zn–O bonds in comparison to that of Mg–O. Indeed, according to empirical bond-type criterion,[17] the resistance to amorphization increases with increasing the ionicity of chemical bonds. Phillip's ionicity of Mg–O and Zn–O bonds are 0.84 and 0.61, respectively.[26] However our results support that this criterion cannot be directly applied for the prediction of damage buildup behavior in ternary compounds.

Finally, we note that the Mg content also affects the substitutional fraction of implanted ions. For example, increasing the Mg content from 0% to 30% leads to reduction in the fraction of incorporated Er atoms in substitutional sites from ~35% to 10% for an ion dose of 5×10^{15} Er/cm^{-2}. Thus, decreasing of substitutional Er is correlated with damage production enhancement which occurs in MgZnO alloy with increasing the Mg content.

C. CdZnO

Figure 5 shows RBS/C spectra illustrating the damage buildup in $Cd_{0.05}Zn_{0.95}O$ films implanted with 200 keV Au^+ ions using two different ion doses as indicated in the legend. The positions of Cd, Zn, and Au at the film surface are indi-

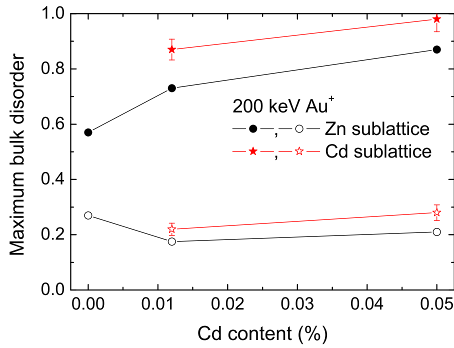

FIG. 6. (Color online) Maximum relative disorder in Zn (dots) and Cd (stars) sublattice as a function of Cd content (x) in $Cd_xZn_{1-x}O$ films implanted at room temperature with 200 keV Au^+ ions to 5×10^{14} cm^{-2} (open symbols) and 5×10^{15} cm^{-2} (closed symbols).

cated in the figure by arrows. It is seen from Fig. 5 that the Au bombardment leads to damage accumulation in both Zn and Cd sublattices and the disorder increases with the ion dose. It is also seen that for the higher dose (5×10^{15} cm^{-2}) the damage level in the Cd sublattice reaches the random RBS level which indicates that all Cd atoms are displaced in the near surface region. On the other hand, our estimations revealed that damage level in the Zn sublattice is lower than that for the Cd sublattice. Thus, the damage accumulation rates in Cd and Zn sublattices in CdZnO are not equal. Such damage accumulation behavior may be attributed to lower effective diffusivity of Cd interstitials in comparison to that of Zn and, consequently, lower efficiency of dynamic annealing in Cd sublattice. This result is in strong contrast to the ternary compounds based on GaN such as InGaN where the implantation disorder proceeds at essentially the same rate.[13] In addition, it should be pointed out that the RBS results also revealed that all Au atoms are localized in nonsubstitutional sites for both ZnO and CdZnO (not shown); this holds even for the low ion dose, in a contrast to the Er implantations in ZnO as discussed in Sec. III B.

The effect of Cd content on the damage buildup is summarized in Fig. 6 showing the maximum bulk disorder in both Zn and Cd sublattices as a function of the Cd content in $Cd_xZn_{1-x}O$ films implanted by Au ions with ion doses of 5×10^{14} cm^{-2} (low) and 5×10^{15} cm^{-2} (high). For pure ZnO, these two doses correspond to the two distinct damage accumulation stages: gradual accumulation (low dose) and saturation (high dose) in accordance with literature (see, for example, Refs. 8 and 20). It is clearly seen from Fig. 6 that increasing the Cd content strongly enhances the damage in both sublattices for high dose implantation. In fact, the damage level in Zn sublattice of high dose implanted CdZnO increases from 0.55 to 0.87 with increasing of the Cd content from 0% to 5% as clearly seen from Fig. 6. This damage level (0.87) is much higher than the saturation level for the bulk damage peak in pure ZnO which is typically $\lesssim 0.5$. However, there is no practically damage enhancement observed for the low ion dose (open symbols in Fig. 6). Furthermore, the implanted ions generate more structural damage in the Cd sublattice than in Zn sublattice, as it is mentioned above and clearly illustrated by the results shown in Fig. 6.

Comparing the damage accumulation in high and low dose implanted samples in Fig. 6 we conclude that the Cd content strongly affects the saturation stage of the damage accumulation behavior. Thus, Cd incorporation in ZnO decreases the dynamic annealing process during ion bombardment. One of the possible reasons for that is the reduced effective diffusivity of Cd and/or Zn interstitials in CdZnO layers. The displaced Cd atoms (or Cd agglomerations) may also act as additional nucleation sites for the defect accumulation and, hence, lead to the damage enhancement in the Zn sublattice of the CdZnO layers. Note that the same mechanism may contribute to the damage enhancement in MgZnO. However, due to the low sensitivity of RBS to light atoms it is not possible to estimate the damage in the Mg sublattice of MgZnO. In addition, the other mechanisms discussed in Sec. III B for enhanced damage accumulation in MgZnO can be also applied to CdZnO. Furthermore, the observed results indicate that CdZnO seems to be less resistant to amorphization than both MgZnO and pure ZnO. Further work is currently pursued to understand the exact role of the Cd atoms in ion-beam-induced damage formation in CdZnO layers.

IV. CONCLUSIONS

In conclusion, we have studied the effect of the film composition on radiation damage accumulation in MgZnO and CdZnO relative to that in pure ZnO. The results show that an increase in either the Mg or Cd contents results in overall enhancement of radiation induced disorder. However, MgZnO as well as pure ZnO exhibit a strong degree of dynamic annealing during implantation and these materials cannot be amorphized even with heavy ion bombardment up to an ion dose of 3×10^{16} Er/cm^2. The incorporation of Cd in ZnO affects the saturation stage of damage accumulation and CdZnO layers seem to be less resistant to amorphization compared to MgZnO or pure ZnO. The observed results may be attributed to: (i) a prominent role of different surface conditions for the interaction with generated point defects in ZnO-based films, relative to pure ZnO; (ii) processes of phase segregation during dynamic annealing; and (iii) enhanced defect accumulation rate for Cd (presumably also for Mg atoms) in W-ZnO-matrix.

ACKNOWLEDGMENTS

Support from the Norwegian Research Council via FRINAT and RENERGI programs is acknowledged. The international cooperation was partially funded by NordForsk and Chinese Academy of Science.

[1] Ü. Özgür, Ya. I. Alivov, C. Liu, A. Teke, M. A. Reshchikov, S. Doğan, V. Avrutin, S.-J. Cho, and H. Morkoç, J. Appl. Phys. **98**, 041301 (2005).
[2] *Thin Films and Nanostructures*, edited by C. Jagadish and S. J. Pearton (Elsevier, Amsterdam, 2006).
[3] T. Makino, Y. Segawa, M. Kawasaki, A. Ohtomo, R. Shiroki, K. Tamura, T. Yasuda, and H. Koinuma, Appl. Phys. Lett. **78**, 1237 (2001).
[4] S. Shigemori, A. Nakamura, J. Ishihara, T. Aoki, and J. Temmyo, Jpn. J. Appl. Phys., Part 2 **43**, L1088 (2004).
[5] F. Bertram, S. Giemsch, D. Forster, J. Christen, R. Kling, C. Kirchner, and

A. Waag, Appl. Phys. Lett. **88**, 061915 (2006).
[6]Z. L. Liu, Z. X. Mei, T. C. Zhang, Y. P. Liu, Y. Guo, X. L. Du, A. Hallen, J. J. Zhu, and A. Yu. Kuznetsov, J. Cryst. Growth **311**, 4356 (2009).
[7]J. L. Morrison, J. Huso, H. Hoeck, E. Casey, J. Mitchell, L. Bergman, and M. G. Norton, J. Appl. Phys. **104**, 123519 (2008).
[8]S. O. Kucheyev, J. S. Williams, C. Jagadish, J. Zou, C. Evans, A. J. Nelson, and A. V. Hamza, Phys. Rev. B **67**, 094115 (2003).
[9]C. W. White, L. A. Boatner, P. S. Sklad, C. J. McHargue, S. J. Pennycook, M. J. Aziz, G. C. Farlow, and J. Rankin, Mater. Res. Soc. Symp. Proc. **74**, 357 (1987).
[10]Z. Q. Chen, M. Maekawa, A. Kawasuso, S. Sakai, and H. Naramoto, J. Appl. Phys. **99**, 093507 (2006).
[11]K. Lorenz, E. Alves, E. Wendler, O. Bilani, W. Wesch, and M. Hayes, Appl. Phys. Lett. **87**, 191904 (2005).
[12]S. O. Kucheyev, J. S. Williams, J. Zou, and C. Jagadish, J. Appl. Phys. **95**, 3048 (2004).
[13]E. Wendler, W. Wesch, E. Alves, and A. Kamarou, Nucl. Instrum. Methods Phys. Res. B **218**, 36 (2004).
[14]Despite that Mg, Cd, and Zn occupy the same type of lattice sites in wurtzite structure of a ternary alloy, we use the term Mg, Cd, and Zn sublattice to distinguish the contributions from different atoms in the damage produced by the ion bombardment in ternary compounds.
[15]K. Schmid, Radiat. Eff. **17**, 201 (1973).
[16]J. F. Ziegler, J. P. Biersack, and U. Littmark, *The Stopping and Range of Ions in Solids* (Pergamon, New York, 1985), Vol. 1, p. 109; www.srim.org
[17]H. M. Naguib and R. Kelly, Radiat. Eff. **25**, 1 (1975).
[18]A. M. Mazzone, Phys. Status Solidi A **95**, 149 (1986).
[19]D. C. Look, G. C. Farlow, P. Reunchan, S. Limpijumnong, S. B. Zhang, and K. Nordlund, Phys. Rev. Lett. **95**, 225502 (2005).
[20]A. Yu. Azarov, S. O. Kucheyev, A. I. Titov, and P. A. Karaseov, J. Appl. Phys. **102**, 083547 (2007).
[21]Note that the Zn depth scale for the MgZnO layers is slightly different from one for the pure ZnO due to different electronic stopping power in these materials. Thus, in order to minimize errors in the depth scale determination for the MgZnO films we calculated electronic stopping power using TRIM code (Ref. 16) with the material density calculated by a linear interpolation between the densities of ZnO ($5.6\ g/cm^3$) and MgO ($3.58\ g/cm^3$).
[22]Note that it is not obvious how to distinguish between the bulk and surface damage peaks in $Mg_{0.3}Zn_{0.7}O$ because of unimodal damage profile. So for these samples the damage levels were chosen at the depth which corresponds to the maximum of relative disorder of bulk damage peak for pure ZnO samples implanted to the same ion dose.
[23]C. Ronning, P. X. Gao, Y. Ding, Z. L. Wang, and D. Schwen, Appl. Phys. Lett. **84**, 783 (2004).
[24]E. Friedland and M. Hayes, Nucl. Instrum. Methods Phys. Res. B **65**, 287 (1992).
[25]E. Wendler, K. Gärtner, and W. Wesch, Nucl. Instrum. Methods Phys. Res. B **266**, 2872 (2008).
[26]C. R. A. Catlow and A. M. Stoneham, J. Phys. C **16**, 4321 (1983).